

Task-Distributionally Robust Data-Free Meta-Learning

Zixuan Hu¹ Li Shen² Zhenyi Wang³ Yongxian Wei¹
Baoyuan Wu⁴ Chun Yuan¹ Dacheng Tao⁵

¹Tsinghua Shenzhen International Graduate School, China; ²JD Explore Academy, China

³University of Maryland, USA; ⁴The Chinese University of Hong Kong, Shenzhen, China

⁵The University of Sydney, Australia

huzixuan21@mails.tsinghua.edu.cn; mathshenli@gmail.com; zwang169@umd.edu

weiyx23@mails.tsinghua.edu.cn; wubaoyuan1987@gmail.com

yuanc@sz.tsinghua.edu.cn; dacheng.tao@gmail.com

Abstract

Data-Free Meta-Learning (DFML) aims to efficiently learn new tasks by leveraging multiple pre-trained models without requiring their original training data. Existing inversion-based DFML methods construct pseudo tasks from a learnable dataset, which is inversely generated from the pre-trained model pool. For the first time, we reveal two major challenges hindering their practical deployments: Task-Distribution Shift (TDS) and Task-Distribution Corruption (TDC). TDS leads to a biased meta-learner because of the skewed task distribution towards newly generated tasks. TDC occurs when untrusted models characterized by misleading labels or poor quality pollute the task distribution. To tackle these issues, we introduce a robust DFML framework that ensures task distributional robustness. We propose to meta-learn from a pseudo task distribution, diversified through task interpolation within a compact task-memory buffer. This approach reduces the meta-learner’s overreliance on newly generated tasks by maintaining consistent performance across a broader range of interpolated memory tasks, thus ensuring its generalization for unseen tasks. Additionally, our framework seamlessly incorporates an automated model selection mechanism into the meta-training phase, parameterizing each model’s reliability as a learnable weight. This is optimized with a policy gradient algorithm inspired by reinforcement learning, effectively addressing the non-differentiable challenge posed by model selection. Comprehensive experiments across various datasets demonstrate the framework’s effectiveness in mitigating TDS and TDC, underscoring its potential to improve DFML in real-world scenarios.

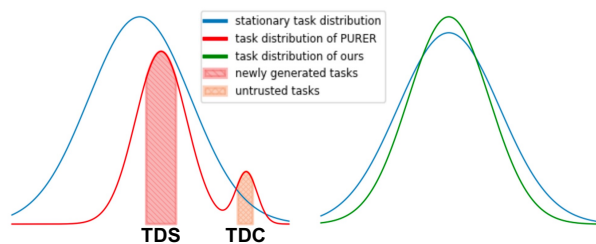


Figure 1. Concepts of TDS and TDC. (Left) At a certain training iteration, TDS occurs when the task distribution skews towards newly generated tasks, deviating from the ideal task distribution. TDC arises from the inclusion of untrusted tasks. (Right) Our framework addresses these issues by meta-learning from a diversified pseudo task distribution that closely mirrors the ideal distribution. This is achieved through task interpolation within a compact memory buffer alongside an automated model selection mechanism.

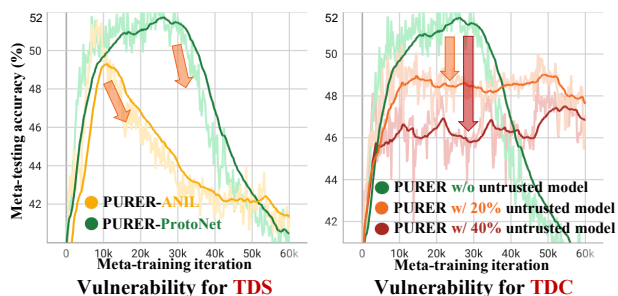


Figure 2. Vulnerabilities of PURER for TDS (left) and TDC (right). “-ANIL” and “-ProtoNet” are two variants of PURER.

1. Introduction

Data-free Meta-learning (DFML) [13, 43], an emerging meta-learning paradigm, gains increasing interest for its ability to reuse multiple pre-trained models to obtain a generalizable meta-learner, without accessing their private training data. This paradigm stands in contrast to traditional meta-

learning [9], which relies heavily on extensive tasks with available training and testing data. One of the most compelling applications of DFML lies in its relevance to real-world scenarios where task-specific data may be unavailable post-training due to constraints like privacy. In such cases, repositories such as GitHub, HuggingFace, and Model Zoo offer numerous pre-trained models without accompanying private training data. DFML provides an effective solution to such scenarios by reusing those pre-trained models without accessing their private training data, to develop a meta-learner with exceptional generalization capabilities for new tasks.

Despite its promise, DFML is not without challenges. Inversion-based DFML methods, for instance, generate pseudo tasks from a dynamically learnable dataset, which is evolved by iteratively querying the pre-trained model pool. For the first time, we reveal two critical issues of existing methods, as illustrated in Fig. 1: Task-Distribution Shift (TDS) and Task-Distribution Corruption (TDC). These issues significantly hinder the practical application of DFML, which has not been explored.

TDS emerges due to the evolving nature of task distributions. PURER [13], the state-of-the-art DFML method, meta-trains on pseudo tasks constructed from a learnable dataset, which is inversely obtained from the pre-trained model pool and evolves adversarially with the meta-learner. This evolution, especially within the adversarial constraints, can skew the task distribution towards newer tasks, resulting in a bias in the meta-learner and a consequent decrease in its generalization for novel tasks. Detailed discussion on PURER is provided in App. D. This phenomenon is evident in Fig. 2, where severe degradation in meta-testing accuracy occurs during PURER’s meta-training phase under the CIFAR-FS 5-way 5-shot setting. This instability is highly undesirable in practical applications, making it difficult to determine the optimal point to terminate meta-training, especially lacking validation set monitoring. Therefore, there is a clear need for a more robust DFML framework. Such a framework should ensure stable accuracy throughout the meta-training process, allowing for a safe termination after a pre-determined sufficient number of iterations.

TDC arises when pre-trained models are sourced from untrusted platforms, which is exemplified in Fig. 3. When employing DFML algorithms to solve rare bird species classification tasks, users actively choose relevant models, such as bird or animal classifiers, as meta-training resources. However, the assumption that all pre-trained models are trustworthy, as posited by PURER [13], is not always valid. Here, we identify two primary risks with untrusted models: those with misleading labels, either due to inaccurate data labeling or deliberate model disguising, and those of low quality, stemming from poor training configurations or inferior training data. Pseudo data generated from models with misleading la-

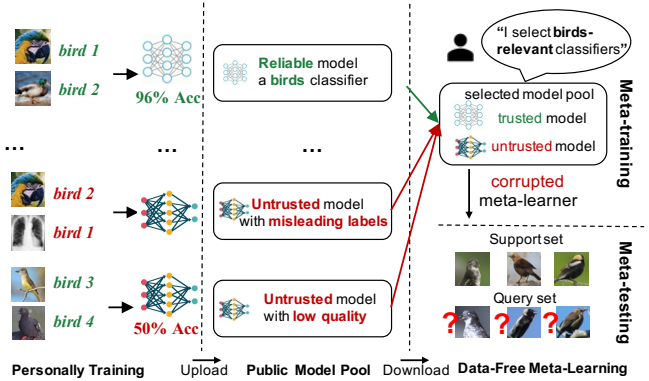


Figure 3. TDC arises due to the use of untrusted pre-trained models, mainly characterized by misleading labels (either due to inaccurate data labeling or deliberate model disguising), or low quality (due to poor training configurations or inferior training data).

els will be inaccurately labeled, causing contradictions with correctly labeled data and thus confusing the meta-learner. Likewise, data generated from low-quality models are often noisy and lacking in discriminative features, thereby hindering the meta-learning process. The significant impact of these untrusted models on PURER is demonstrated through a case study in Fig. 2 under the CIFAR-FS 5-way 5-shot setting. In this case, these untrusted models, while claimed to be from CIFAR-FS, are actually trained on diverse datasets including EuroSAT, ISIC, ChestX, Omniglot, and MNIST. Addressing this issue by individually assessing each model’s reliability through gathering specific testing data, though straightforward, is impractical in DFML scenarios, given the vast number of pre-trained models and associated constraints like time, resources, and privacy. Therefore, we advocate for the development of an efficient, automated method to identify and utilize reliable models from a large pool without necessitating extensive individual model testing.

To address TDS and TDC, for the first time, we develop a novel DFML framework that ensures task distributional robustness. Our framework leverages meta-learning from a pseudo task distribution, which is diversified through task interpolation over a compact task-memory buffer. This prevents the meta-learner from over-relying on newly generated tasks by maintaining stable performance across a broader range of interpolated past tasks, thus ensuring its generalization for unseen tasks. We present two practical implementations of task interpolation, including task-level *combination* and *mixup*. The implementation of task interpolation is flexible, with many potential extensions for future research. Furthermore, our framework seamlessly incorporates an automated model selection mechanism within the meta-training process, parameterizing each model’s reliability as a learnable weight. We employ a policy gradient algorithm from reinforcement learning to optimize these weights, regarding the meta-learner’s performance on held-out unseen tasks as

rewards, which effectively addresses the non-differentiable challenge posed by model selection. This selection mechanism is also designed to be versatile and compatible with existing DFML methods to alleviate TDC. Our contributions are validated through extensive experiments across multiple datasets, which confirms the efficacy of our framework in mitigating the TDS and TDC issues, and underscores its applicability in real-world DFML deployments. We outline our contributions as follows:

- For the first time, we reveal the vulnerabilities of existing DFML methods to TDS and TDC, highlighting the critical need for robust DFML deployments in real-world applications.
- We introduce a novel DFML framework ensuring task distributional robustness, featuring a diversified pseudo task distribution through task interpolation over a memory buffer and an automated model selection mechanism.
- We provide empirical evidence across various datasets to verify our framework’s effectiveness in addressing TDS and TDC, indicating its utility in enhancing the practical deployment of DFML.

2. Related Work

Data-Free Meta-Learning (DFML) is a novel approach designed to facilitate the efficient learning of new tasks through meta-learning from pre-trained models, without the need for original training data. In contrast to traditional data-based meta-learning methods [10, 11, 14, 16, 22, 27, 30, 32, 45, 47–49, 51] that rely on large datasets, DFML offers a solution to obtain a meta-learner with superior generalization ability from a collection of task-specific pre-trained models with weaker generalization ability. The concept of DFML, first introduced by Wang et al. [43], involves meta-learning a hyper-network that takes pre-trained models as inputs and directly outputs a fused model. A more advanced method, recently proposed by Hu et al. [13], utilizes inversion-based techniques to significantly enhance performance. Their approach, known as PURER, constructs pseudo tasks from a learnable dataset inversely generated from the pre-trained model pool. However, these approaches often assume the reliability of all pre-trained models and overlook the evolving nature of iteratively generated tasks, leaving them susceptible to TDS and TDC. Our work is the first to highlight these vulnerabilities in inversion-based DFML methods and emphasize the need for robust solutions.

Data-free learning. This concept focuses on learning processes that operate without real data access, an important consideration in scenarios where data availability is constrained [53, 54, 56]. An example of data-free learning is the vanilla model average and its variants, which only utilize the parameters and architectures of pre-trained models. Recent advancements in model inversion techniques

[2, 2, 4, 6–8, 17, 23–25, 34, 40, 52, 55] have propelled this field forward, allowing for the synthesis of pseudo data from pre-trained models. Nonetheless, these methods often overlook challenges such as non-stationary data distributions and the assumption of model reliability.

Distributional robustness in meta-learning. The field of meta-learning has introduced some methods to address the sequential task-distribution shift in meta-learning [11, 29]. Other methods [15, 18, 21, 33, 37, 41, 42, 46] aim to enable effective meta-learning in scenarios with heterogeneous task distributions. However, all these solutions are predominantly aligned with data-based meta-learning, but the unique challenges of distributional robustness in the context of data-free meta-learning remain unexplored and unaddressed.

3. Methodology

In this section, we introduce a novel DFML framework ensuring task distribution robustness, featuring a diversified pseudo task distribution through task interpolation over a memory buffer (Sec. 3.2) and an automated model selection mechanism (Sec. 3.3). Below, we begin with the basic problem setup of DFML.

3.1. Problem Setup of DFML

Meta-training. In the context of DFML, we are given a collection of pre-trained models $\mathcal{M}_{\text{pool}}$, where each model $M \in \mathcal{M}_{\text{pool}}$ is tailored to specific tasks. The aim is to meta-learn a meta-learner $\mathcal{A}[\cdot; \theta_{\mathcal{A}}]$ using $\mathcal{M}_{\text{pool}}$, enabling rapid adaptation to new unseen tasks $\mathcal{T}_{\text{test}}$. We highlight that the models in $\mathcal{M}_{\text{pool}}$ may possess heterogeneous architectures. In line with standard meta-learning protocols, we can engage with a limited number of validation tasks, ensuring their label spaces do not overlap with those of the meta-training models or the meta-testing tasks.

Meta-testing. We evaluate the meta-learner on 600 unseen N -way K -shot tasks. The classes encountered during the meta-testing phase have never been seen during the meta-training phase or in the validation tasks. Each task $\mathcal{T}_{\text{test}} = (\mathbf{D}_{\text{test}}^{\text{s}}, \mathbf{D}_{\text{test}}^{\text{q}})$ consists of a support set $\mathbf{D}_{\text{test}}^{\text{s}} = (\mathbf{X}_{\text{test}}^{\text{s}}, \mathbf{Y}_{\text{test}}^{\text{s}})$ with N classes and K instances per class. We utilize the support set $\mathbf{D}_{\text{test}}^{\text{s}}$ to adapt the meta learner parameterized by $\theta_{\mathcal{A}}$ to obtain the task-specific solver $\mathcal{A}[\mathbf{D}_{\text{test}}^{\text{s}}; \theta_{\mathcal{A}}]$ and make predictions on its query set $\mathbf{D}_{\text{test}}^{\text{q}}$. The overall accuracy is measured by averaging the accuracies across all the meta-testing tasks.

3.2. Diversified Pseudo Task Distribution (SPAN)

The DFML objective is formulated to optimize the meta-learner, parameterized by $\theta_{\mathcal{A}}$, by minimizing the expected loss over a pseudo task distribution $\hat{p}_{\mathcal{T}}$:

$$\min_{\theta_{\mathcal{A}}} \mathbb{E}_{\hat{\mathcal{T}} \in \hat{p}_{\mathcal{T}}} \mathcal{L}_{\text{task}} \left(\hat{\mathbf{D}}^{\text{q}}; \mathcal{A}[\hat{\mathbf{D}}^{\text{s}}; \theta_{\mathcal{A}}] \right), \quad (1)$$

where $\hat{\mathcal{T}}$ represents a pseudo task comprising a support set $\hat{\mathbf{D}}^s$ and a query set $\hat{\mathbf{D}}^q$, sampled from $\hat{p}_{\mathcal{T}}$. The meta-learner could be entirely shared across tasks in metric-based methods like ProtoNet [31], or partially in gradient-based methods like MAML, where only layers before the classification head are shared across tasks. The task-specific adaptation on non-shared parts uses the support set $\hat{\mathbf{D}}^s$, which can be implemented through various approaches such as in-context (black-box) learning [3], gradient optimization [9] and metric learning [31]. We use $\mathcal{A}[\hat{\mathbf{D}}^s; \theta_{\mathcal{A}}]$ denote the adaption process on $\theta_{\mathcal{A}}$ using $\hat{\mathbf{D}}^s$. The task-level loss function $\mathcal{L}_{\text{task}}(\cdot)$ assesses the effectiveness of the adapted model on the query set $\hat{\mathbf{D}}^q$. The ultimate aim is to train the meta-learner for effective adaptation to a diverse range of tasks from $\hat{p}_{\mathcal{T}}$, thereby enhancing its generalization to unseen tasks.

We tackle the challenge of approximating the task distribution $\hat{p}_{\mathcal{T}}$ by inversely generating pseudo tasks from each pre-trained model M . This is achieved by iteratively querying the model and employing a conditional generator $G(\cdot; \theta_G)$, initially randomly initialized for each model. The generator takes standard Gaussian noise \mathbf{Z} and predefined target label $\hat{\mathbf{Y}}$ as inputs, to produce the generated data $\hat{\mathbf{X}} = G(\mathbf{Z}, \hat{\mathbf{Y}}; \theta_G)$. The generator’s optimization is driven by the feedback or loss obtained after inputting $\hat{\mathbf{X}}$ into M , aiming to minimize the cross-entropy loss \mathcal{L}_{CE} with the target labels $\hat{\mathbf{Y}}$ that can be represented as either hard labels (e.g., [1, 0, 0]) or soft labels (e.g., [0.7, 0.1, 0.2]). The generation objective is formulated as:

$$\min_{\theta_G} \mathcal{L}_{\text{CE}}(\hat{\mathbf{X}}, \hat{\mathbf{Y}}; \theta_G) = \min_{\theta_G} \text{CE}(M(\hat{\mathbf{X}}), \hat{\mathbf{Y}}). \quad (2)$$

To fill the gap between generated and original training data, we incorporate a regularization term following [50]. This term ensures that the feature-map statistics of the generated data align with those of the original training data, as stored in the BatchNormalization (BN) layers of the pre-trained models:

$$\mathcal{L}_{\text{BN}}(\hat{\mathbf{X}}; \theta_G) = \sum_l \|\mu_l(\hat{\mathbf{X}}) - \mu_l^{\text{BN}}\| + \|\sigma_l^2(\hat{\mathbf{X}}) - \sigma_l^{\text{BN}}\|. \quad (3)$$

Here, $\hat{\mathbf{X}}$ represents a batch of generated data and μ_l and σ_l^2 denote their mean and variance at the l^{th} convolutional layer. μ_l^{BN} and σ_l^{BN} refer to the mean and variance of original training data stored in the l^{th} BN layer. Combining these terms, we define the generator’s optimization process as:

$$\min_{\theta_G} \mathcal{L}_G(\mathbf{Z}, \hat{\mathbf{Y}}; \theta_G) = \mathcal{L}_{\text{CE}} + \mathcal{L}_{\text{BN}}. \quad (4)$$

To construct the pseudo task $\hat{\mathcal{T}}$, we select $\hat{\mathbf{X}}$ that yields the minimum \mathcal{L}_G during the optimization of θ_G , and then randomly split $(\hat{\mathbf{X}}, \hat{\mathbf{Y}})$ into a support set $\hat{\mathbf{D}}^s = (\hat{\mathbf{X}}^s, \hat{\mathbf{Y}}^s)$ and a query set $\hat{\mathbf{D}}^q = (\hat{\mathbf{X}}^q, \hat{\mathbf{Y}}^q)$. The task generation process is detailed in App. B.

Task interpolation within memory buffer. To avoid over-reliance on newly generated tasks, we diversify the pseudo task distribution $\hat{p}_{\mathcal{T}}$ through task interpolation over a compact task-memory buffer. The memory buffer is implemented via reservoir sampling (RS), similar to [28]. This interpolation across memory tasks broadens the range of tasks for meta-training, essential for effective meta-learning, without the need for exceeding the memory buffer or requiring extensive pre-trained models. Here, we present two practical implementations of task interpolation, including task-level *combination* and *mixup* [48]. (i) *Combination* refers to combining different classes from multiple memory tasks to form a new task. For example, from two 2-way memory tasks with label spaces of (i_1, i_2) and (j_1, j_2) , an interpolated task could be (i_1, j_2) ; (ii) *Mixup* interpolates tasks by blending hidden representations. Using the previous example, an interpolated 2-way task could be (e_1, e_2) , where e_1 and e_2 are new labels for interpolated classes. The mixup is conducted on hidden representations of one certain layer shared across tasks in the meta-learner. For MAML without task-shared layers, mixup is allowed on the inputs. For instance, to construct the new class e_1 , we first randomly select one layer l shared across tasks, and then apply mixup on its hidden representations of classes i_1 and j_2 , i.e. $\mathbf{h}_{e_1}^{(l)} = \lambda \mathbf{h}_{i_1}^{(l)} + (1 - \lambda) \mathbf{h}_{j_2}^{(l)}$, with $\lambda \in [0, 1]$ sampled from a Beta distribution $\text{Beta}(\alpha, \beta)$. Also, the implementation for task interpolation is flexible and can be further explored in future works. Empirically, a *hybrid* approach combining *combination* and *mixup* yields superior performance due to the generation of more diverse tasks with varying difficulty levels, which is also evidenced through t-SNE visualization in App. E.

Different choices of $\mathcal{L}_{\text{task}}$ for new tasks and interpolated memory tasks. For newly generated tasks, we employ a distillation loss, minimizing the Kullback–Leibler (KL) divergence between the predictions of the meta-learner and the pre-trained model. This approach leverages the rich supervision available from the pre-trained model. For interpolated memory tasks, we use a cross-entropy loss against hard labels, given the mismatch between label spaces of interpolated tasks and those of the pre-trained models:

$$\theta_{\mathcal{A}}^{(k+1)} \leftarrow \begin{cases} \theta_{\mathcal{A}}^{(k)} - \nabla_{\theta_{\mathcal{A}}^{(k)}} \text{KL} \left(\mathcal{A}[\hat{\mathbf{D}}^s; \theta_{\mathcal{A}}](\hat{\mathbf{X}}^q), M(\hat{\mathbf{X}}^q) \right) \\ \theta_{\mathcal{A}}^{(k)} - \nabla_{\theta_{\mathcal{A}}^{(k)}} \text{CE} \left(\mathcal{A}[\hat{\mathbf{D}}^s; \theta_{\mathcal{A}}](\hat{\mathbf{X}}^q), \hat{\mathbf{Y}}^q \right) \end{cases} \quad (5)$$

Flexible choice of the meta-learner \mathcal{A} . Our proposed DFML framework is compatible to both optimization-based (e.g. MAML [9]), and metric-based meta-learning algorithms (e.g. ProtoNet [31]). For instance, in MAML, the meta-learner adapts through gradient descent on the support set \mathbf{D}^s to produce a task-specific model F :

$$\begin{aligned} \mathcal{A}_{\text{MAML}}[\mathbf{D}^s; \theta_{\mathcal{A}}](\mathbf{X}^q) &= F(\mathbf{X}^q; \psi), \\ \text{s.t. } \psi &= \theta_{\mathcal{A}} - \nabla_{\theta_{\mathcal{A}}} \text{CE}(F(\mathbf{X}^s; \theta_{\mathcal{A}}), \mathbf{Y}^s) \end{aligned} \quad (6)$$

For ProtoNet, the meta-learner functions as a feature extractor denoted $f(\cdot; \theta_{\mathcal{A}})$. It assigns labels to the query set \mathbf{X}^q based on the nearest class center in the feature space. The probability of a query example being classified into class c is calculated as:

$$[\mathcal{A}_{\text{ProtoNet}}[\mathbf{X}^s; \theta_{\mathcal{A}}](\mathbf{X}^q)]_c = \frac{\exp(-\|f(\mathbf{X}^q; \theta_{\mathcal{A}}) - \mathbf{C}_c\|)}{\sum_{c'} \exp(-\|f(\mathbf{X}^q; \theta_{\mathcal{A}}) - \mathbf{C}_{c'}\|)}, \quad (7)$$

where the class center \mathbf{C}_c is the average feature embedding in \mathbf{D}^s of class c .

3.3. Automated Model Selection (AMS)

We incorporate an automated model selection mechanism within the meta-training process to ensure robust model selection. We parameterize models' reliability as a learnable weight vector $\mathbf{W} \in \mathbb{R}^{|\mathcal{M}_{\text{pool}}|}$, where w_i characterizes the reliability of M_i from the model pool $\mathcal{M}_{\text{pool}}$. At each iteration, we take an action selecting a batch of models $\mathcal{M}_{\text{select}}$ with the highest weights from $\mathcal{M}_{\text{pool}}$. We use $\pi(\mathcal{M}_{\text{select}}|\mathcal{M}_{\text{pool}}; \mathbf{W})$ to denote the probability of taking this action, *i.e.* selecting $\mathcal{M}_{\text{select}}$ from $\mathcal{M}_{\text{pool}}$:

$$\pi(\mathcal{M}_{\text{select}}|\mathcal{M}_{\text{pool}}; \mathbf{W}) = \prod_{i \in \text{INDEX}(\mathcal{M}_{\text{select}})} \left(\frac{e^{w_i}}{\sum_{i'=1}^{|\mathcal{M}_{\text{pool}}|} e^{w_{i'}}} \right), \quad (8)$$

where $\text{INDEX}(\mathcal{M}_{\text{select}})$ returns the entry indexes of $\mathcal{M}_{\text{select}}$ in $\mathcal{M}_{\text{pool}}$. An alternative way to model the selection policy is to adopt a neural network, which can be viewed as further works. The goal of each selection is to optimize the meta-learner's generalization performance on a minimal set of validation tasks $\mathcal{T}_v^{\text{val}} = (\mathbf{D}_v^{\text{val},s}, \mathbf{D}_v^{\text{val},q})$, *i.e.* the meta-learner meta-trained with the selected models $\mathcal{M}_{\text{select}}$ can generalize well to held-out unseen tasks. We argue that we only need a minimal set of validation tasks (only two in our case), which is substantially fewer than the extensive task sets typically required for meta-training. The objective is formulated as follows:

$$\min_{\mathbf{W}} \frac{1}{N_v} \sum_{v=1}^{N_v} \mathcal{L}_{\text{task}} \left(\mathbf{D}_v^{\text{val},q}; \mathcal{A}[\mathbf{D}_v^{\text{val},s}; \theta_{\mathcal{A}}^*(\mathbf{W})] \right), \quad (9)$$

where $\theta_{\mathcal{A}}^* = \text{DFML}(\mathcal{M}_{\text{select}}; \mathbf{W})$,

where $\text{DFML}(\mathcal{M}_{\text{select}})$ return the meta-learner trained with selected models via Eq. (5).

Optimization via RL. The model selection operation (*i.e.*, $\mathcal{M}_{\text{select}} \leftarrow \mathcal{M}_{\text{pool}}$) is non-differentiable, making the optimization Eq. (9) intractable. Therefore, we adopt the REINFORCE policy gradient method [44] to reformulate Eq. (9) to a differentiable form Eq. (10). Specifically, at meta-iteration k , we regard the average accuracy on N_v validation tasks as rewards $\sum_{v=1}^{N_v} R_v^{(k)}$. Intuitively, if the action $\mathcal{M}_{\text{select}}^{(k)} \leftarrow \mathcal{M}_{\text{pool}}$ leads to an increasing reward, we will optimize the policy to increase the probability of taking this

Algorithm 1: OVERALL FRAMEWORK

```

1 Input: Pre-trained model pool  $\mathcal{M}_{\text{pool}}$ ; generator  $G(\cdot; \theta_G)$ ;
   meta-learner  $\mathcal{A}[\cdot; \theta_{\mathcal{A}}^{(0)}]$ ; memory buffer  $\mathcal{B}$ ; threshold  $p_s$ .
2 Output: Meta-learner  $\theta_{\mathcal{A}}$ 
3 Randomly initialize  $\theta_{\mathcal{A}}^{(0)}$  and reliability weights  $\mathbf{W}^{(0)}$ 
4 Clear memory bank  $\mathcal{B} \leftarrow []$ 
5 for each meta-iteration  $k \leftarrow 0$  to  $N$  do
6    $p \leftarrow \text{random.uniform}(0, 1)$ 
7   if  $p < p_s$  then
8     // automated model selection
9      $\mathbf{P}^{(k)} \leftarrow \text{SoftMax}(\mathbf{W}^{(k)})$ 
10    Select a batch of models  $\mathcal{M}_{\text{select}}$  based on  $\mathbf{P}^{(k)}$ 
11    // meta-train on new tasks
12    Generate a batch of pseudo tasks  $\hat{\mathcal{T}}$ 
13    Update memory buffer via reservoir sampling
14    Update  $\theta_{\mathcal{A}}^{(k+1)} \leftarrow \theta_{\mathcal{A}}^{(k)}$  via Eq. (5)
15    Calculate rewards of  $\theta_{\mathcal{A}}^{(k+1)}$  on  $\mathcal{T}^{\text{val}}$ 
16    Update  $\mathbf{W}^{(k+1)} \leftarrow \mathbf{W}^{(k)}$  via Eq. (10)
17  else
18    // meta-train on memory
19    Construct a batch of interpolated tasks  $\tilde{\mathcal{T}}$  from  $\mathcal{B}$ 
20    Update  $\theta_{\mathcal{A}}^{(k+1)} \leftarrow \theta_{\mathcal{A}}^{(k)}$  via Eq. (5)

```

action $\pi(\mathcal{M}_{\text{select}}^{(k)}|\mathcal{M}_{\text{pool}})$, and vice versa. To reduce the gradient variance and stabilize the optimization process, we introduce the baseline function b as the moving average of all past rewards:

$$\begin{aligned} \mathbf{W}^{(k+1)} &\leftarrow \mathbf{W}^{(k)} + \\ \nabla_{\mathbf{W}^{(k)}} &\left[\log \pi(\mathcal{M}_{\text{select}}^{(k)}|\mathcal{M}_{\text{pool}}; \mathbf{W}^{(k)}) \times \left(\frac{1}{N_v} \sum_{v=1}^{N_v} R_v^{(k)} - b \right) \right]. \end{aligned} \quad (10)$$

This RL-based optimization approach ensures dynamic identification and selection of reliable models. We provide an overall framework in Alg. 1.

4. Experiments

In this section, we provide empirical evidence across various datasets to verify our framework's effectiveness.

Experimental setup. Our experiments utilized four datasets: CIFAR-FS [1], MiniImageNet [36], VGG-Flower [26], and CUB-200-2011 (CUB) [38], ranging from general natural images to specific categories like birds (CUB) and flowers (VGG-Flower). Following standard splits [33], we split each dataset into meta-training, meta-validating and meta-testing subsets with disjoint label spaces. Following Wang et al. [43] and Hu et al. [13], we collect 100 models pre-trained on 100 N -way tasks sampled from the meta-training subset, while the meta-learner is finally evaluated on 600 tasks sampled from the meta-testing subset. The meta-learner

Table 1. Results of DFML with trusted models. † denotes our proposed framework.

Method	CIFAR-FS [1]				MiniImageNet [36]			
	5-way 1-shot		5-way 5-shot		5-way 1-shot		5-way 5-shot	
	PEAK	LAST	PEAK	LAST	PEAK	LAST	PEAK	LAST
RANDOM	28.59 ± 0.56	28.59 ± 0.56	34.77 ± 0.62	34.77 ± 0.62	25.06 ± 0.50	25.06 ± 0.50	28.10 ± 0.52	28.10 ± 0.52
AVERAGE	23.96 ± 0.53	23.96 ± 0.53	27.04 ± 0.51	27.04 ± 0.51	23.79 ± 0.48	23.79 ± 0.48	27.49 ± 0.50	27.49 ± 0.50
DRO	30.43 ± 0.43	29.35 ± 0.41	36.21 ± 0.51	35.28 ± 0.49	27.56 ± 0.48	25.22 ± 0.42	30.19 ± 0.43	28.43 ± 0.44
PURER-ANIL	35.31 ± 0.70	26.40 ± 0.43	51.63 ± 0.78	41.24 ± 0.68	30.20 ± 0.61	23.05 ± 0.36	40.78 ± 0.62	29.60 ± 0.53
PURER-ProtoNet	36.26 ± 0.62	27.01 ± 0.58	52.67 ± 0.68	40.53 ± 0.67	30.46 ± 0.64	24.00 ± 0.52	41.00 ± 0.58	31.32 ± 0.52
SPAN-ANIL†	40.39 ± 0.79	39.69 ± 0.79	55.31 ± 0.75	52.92 ± 0.75	32.58 ± 0.68	29.76 ± 0.61	43.63 ± 0.72	42.45 ± 0.67
SPAN-ProtoNet†	40.80 ± 0.78	40.28 ± 0.79	57.11 ± 0.78	55.69 ± 0.76	32.61 ± 0.64	31.97 ± 0.61	42.93 ± 0.65	41.28 ± 0.64

Method	VGG-Flower [26]				CUB [38]			
	5-way 1-shot		5-way 5-shot		5-way 1-shot		5-way 5-shot	
	PEAK	LAST	PEAK	LAST	PEAK	LAST	PEAK	LAST
RANDOM	38.39 ± 0.71	38.39 ± 0.71	48.18 ± 0.65	48.18 ± 0.65	26.26 ± 0.48	26.26 ± 0.48	29.89 ± 0.55	29.89 ± 0.55
AVERAGE	24.52 ± 0.46	24.52 ± 0.46	32.78 ± 0.53	32.78 ± 0.53	24.53 ± 0.46	24.53 ± 0.46	28.00 ± 0.47	28.00 ± 0.47
DRO	40.02 ± 0.72	38.98 ± 0.74	50.22 ± 0.68	49.13 ± 0.70	28.33 ± 0.69	26.01 ± 0.68	31.24 ± 0.76	29.39 ± 0.70
PURER-ANIL	51.34 ± 0.80	45.02 ± 0.68	67.26 ± 0.75	62.54 ± 0.72	31.29 ± 0.64	25.05 ± 0.62	43.34 ± 0.59	32.08 ± 0.60
PURER-ProtoNet	53.90 ± 0.76	47.12 ± 0.71	68.01 ± 0.68	64.51 ± 0.67	31.62 ± 0.63	27.23 ± 0.61	45.36 ± 0.71	35.32 ± 0.66
SPAN-ANIL†	55.28 ± 0.79	54.86 ± 0.76	69.03 ± 0.78	68.52 ± 0.75	35.65 ± 0.72	34.32 ± 0.69	47.24 ± 0.72	46.28 ± 0.65
SPAN-ProtoNet†	57.31 ± 0.85	56.79 ± 0.80	71.12 ± 0.71	70.60 ± 0.69	37.47 ± 0.73	36.67 ± 0.71	48.68 ± 0.71	47.64 ± 0.68

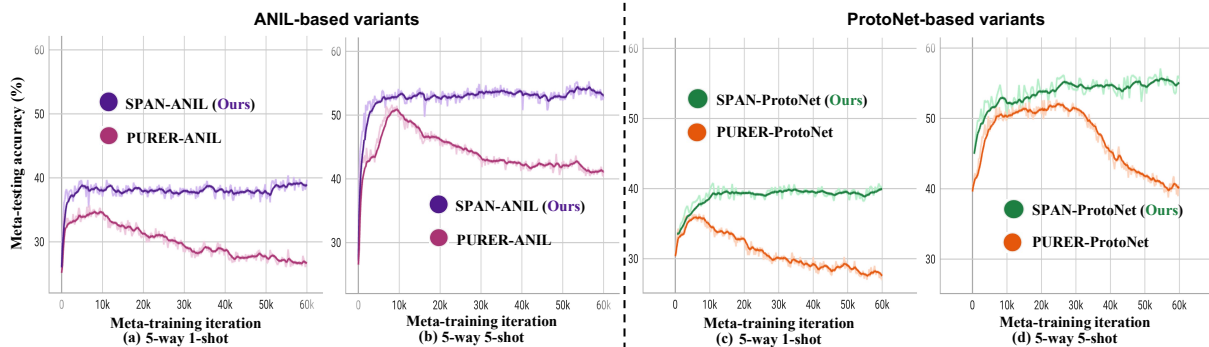


Figure 4. Stability comparison is SPAN versus PURER across 60K meta-training iterations. This figure illustrates the superiority of SPAN, highlighting its significantly higher and more stable meta-testing accuracy throughout the entire meta-training phase.

and pre-trained models employ a Conv4 architecture for consistency with existing works. Hyperparameters included an inner learning rate of 0.01 and an outer learning rate of 0.001 for SPAN-ANIL, and a learning rate of 0.001 for SPAN-ProtoNet. The threshold p_s is empirically set as 0.4. The memory bank was limited to 20 tasks. The structure of the generator and other setup is detailed in App. C and App. A. If not otherwise specified, we use *combination* for task interpolation.

Baselines. (i) **RANDOM.** Training a classifier from scratch using the support set for each meta-testing task. (ii) **AVERAGE.** Average all pre-trained models and then fine-tune the average one using the support set. (iii) **DRO** [43]. Meta-learn a hyper-network to fuse all pre-trained models into one single model, which is then fine-tuned using the support set for each meta-testing task. (iv) **PURER-[.]** [13]. Adversarially train the meta-learner with a learnable dataset inversely generated from pre-trained models. [.] represents the meta-learning algorithm used, such as ANIL or ProtoNet.

Metrics. (i) **PEAK** denotes the peak meta-testing accuracy obtained by the checkpoints with the highest meta-validating accuracy. (ii) **LAST** denotes the meta-testing accuracy at the final iteration. (iii) **VARIATION** denotes the value of “LAST - PEAK”, indicating the stability of performance.

4.1. DFML with Trusted Models

In this subsection, we first explore our proposed framework’s efficacy when meta-trained exclusively with trusted models, establishing a basic understanding of our framework’s capability in such an ideal training scenario.

Results & Analysis. Tab. 1 shows results for 5-way classification compared with existing baselines. We list our main findings as follows: (i) SPAN achieve significantly higher PEAK accuracy across all four datasets. Compared with the best baseline, SPAN achieves 2.15% ~ 5.85% performance gains for 1-shot learning and 2.63% ~ 4.44% gains for 5-shot learning w.r.t. the PEAK accuracy. (ii) SPAN achieve significantly higher LAST accuracy and less VARIATION across

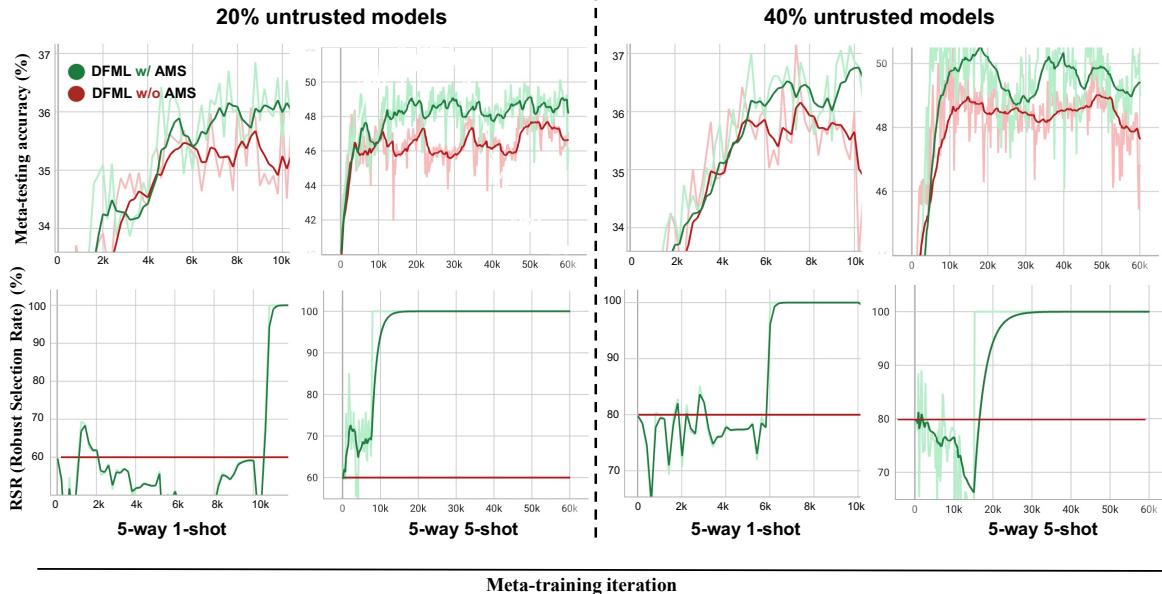


Figure 5. (Top) Performance Improvements with AMS on CIFAR-FS. (Bottom) Increasing trends in RSR indicate AMS’s enhanced capability in identifying reliable models and filtering out unreliable ones over time.

all four datasets. Compared with the best baseline, SPAN achieves 6.75% ~ 10.93% performance gains for 1-shot learning and 6.09% ~ 14.45% gains for 5-shot learning w.r.t. the LAST accuracy. As Fig. 4 indicates, SPAN maintains stable meta-testing accuracy throughout 60k meta-training iterations, contrasting sharply with PURER’s significant performance degradation due to its over-reliance on new tasks and consequent overfitting. (iii) Simply AVERAGE all models, surprisingly, even performs worse than RANDOM. This is attributed to the lack of alignment in the parameter space among models trained on different tasks. Further analysis in Tab. 6 explores the sensitivity of AVERAGE to the number of pre-trained models.

4.2. DFML with Untrusted Models

In this subsection, we further explore our proposed framework’s robustness when exposed to untrusted models within the training model pool. The setup and results of this exploration are detailed below.

Setup of untrusted models. We integrated a set of untrusted models into the training model pool to assess the robustness of the DFML framework. These untrusted models are sourced from various datasets including EuroSAT [12], ISIC [5, 35], ChestX [39], Omniglot [19] and MNIST [20], but are attached with labels from CIFAR-FS. The extent of this integration was measured using a metric termed “pollution rate”, which quantifies the proportion of untrusted models in the pool. Further experiments, focusing on different forms of untrusted models such as low-quality models, are detailed in App. E.

Results & Analysis. Table Tab. 2 demonstrates that the

Table 2. DFML w/ untrusted models across various pollution rates.

Pollution Rate	Method	5-way 1-shot	5-way 5-shot
10%	SPAN	34.37 ± 0.71	47.51 ± 0.72
	SPAN + AMS	35.57 ± 0.67 ^{+1.20%}	49.34 ± 0.72 ^{+1.83%}
20%	SPAN	33.12 ± 0.69	46.79 ± 0.72
	SPAN + AMS	34.24 ± 0.69 ^{+1.12%}	48.72 ± 0.74 ^{+1.93%}
40%	SPAN	33.03 ± 0.71	45.25 ± 0.74
	SPAN + AMS	35.22 ± 0.75 ^{+2.19%}	46.81 ± 0.74 ^{+1.56%}
60%	SPAN	31.20 ± 0.68	42.65 ± 0.72
	SPAN + AMS	33.17 ± 0.66 ^{+1.97%}	45.60 ± 0.69 ^{+2.95%}
80%	SPAN	30.47 ± 0.64	40.96 ± 0.70
	SPAN + AMS	33.06 ± 0.68 ^{+2.59%}	43.58 ± 0.65 ^{+2.62%}

automated model selection (AMS) mechanism consistently improves performance across various pollution rates (from 10% to 80%) on CIFAR-FS. This is evident with gains of 1.12% to 2.59% in 1-shot learning and 1.56% to 2.95% in 5-shot learning. Notably, as the pollution rate increases, AMS demonstrates more significant improvements, suggesting that involving AMS does improve the robustness of DFML. Additional tests on other DFML methods like PURER (refer to App. E) further demonstrate the versatility of AMS.

Analysis of reliability weights. To understand the inner workings of AMS, we take a deep look at the trend of those learnable reliability weights \mathbf{W} during the meta-training phase. We introduced an indicator named Robust Sampling Rate (RSR) for this analysis:
$$\text{RSR} = \sum_{i \in \text{INDEX}(\mathcal{M}_{\text{trust}})} \left(\frac{e^{w_i}}{\sum_{i'=1}^{|\mathcal{M}_{\text{pool}}|} e^{w_{i'}}} \right)$$
, where $\text{INDEX}(\mathcal{M}_{\text{benign}})$ returns the entry indexes of all trusted models $\mathcal{M}_{\text{trust}}$ in $\mathcal{M}_{\text{pool}}$. RSR essentially reflects the likelihood of selecting trusted models. An upward trend in RSR values, as depicted in Fig. 5 (Bottom), indicates that AMS

progressively improves at distinguishing and filtering out untrusted models, increasingly favoring trusted ones as the meta-training process goes on.

4.3. Ablation Studies

Effect of each component. Tab. 3 analyzes the effectiveness of each component¹. The “Vanilla” (V) approach, which utilizes pseudo tasks synthesized from models without a memory buffer, exhibits significant performance degradation due to the TDS issue. Merely incorporating a Memory buffer (M) into the framework does not yield substantial benefits. This limited impact is attributed to the insufficient diversity in task distribution, which fails to adequately prepare the meta-learner for generalizing to unseen tasks. The addition of task Interpolation (I) results in significantly higher peak performance and reduced variation. This improvement underscores the pivotal role of the interpolation mechanism in enhancing robustness and boosting generalization capabilities. Implementing Soft-label (denoted as S) supervision from pre-trained models (Eq. (5)) further enhances the framework’s performance. With all components, we achieve the best with a boosting improvement, demonstrating the effectiveness of the joint schema.

Table 3. Effect of each component.

Method	5-way 1-shot		5-way 5-shot	
	PEAK	LAST	PEAK	LAST
V	35.34 ± 0.68	26.76 ± 0.64	50.31 ± 0.72	39.22 ± 0.74
V + M	36.02 ± 0.70	28.33 ± 0.68	51.23 ± 0.72	41.54 ± 0.70
V + M + I	38.76 ± 0.74	38.42 ± 0.72	54.91 ± 0.74	53.52 ± 0.74
V + M + I + S	40.80 ± 0.78	40.28 ± 0.79	57.11 ± 0.78	55.69 ± 0.76

Variants of task interpolation. As shown in Tab. 4, solely using *mixup* is suboptimal because tasks interpolated by *mixup* tend to be more “difficult” compared with *combination*, making them less effective for meta-training purposes. We adopt a hybrid strategy that applies different interpolation methods with varying probabilities, which ensures a more diverse task distribution spanning a broader range of difficulty levels, thereby enhancing the overall generalization. T-SNE visualizations of pseudo tasks in App. E corroborate our findings and offer a deeper understanding of how different interpolation strategies influence task difficulty and diversity.

Table 4. Variants of task interpolation.

Interpolation Method	5-way 1-shot		5-way 5-shot	
	PEAK	LAST	PEAK	LAST
combination	40.80 ± 0.78	40.28 ± 0.79	57.11 ± 0.78	55.69 ± 0.76
mixup	39.67 ± 0.76	39.04 ± 0.77	54.02 ± 0.78	53.19 ± 0.75
80% combination+20% mixup	41.43 ± 0.75	41.02 ± 0.76	58.21 ± 0.76	57.62 ± 0.77

Effect of the budgets of memory buffer. Tab. 5 shows the effect of the memory buffer size. With the incorporation of

¹If no otherwise specified, experiments in Sec. 4.3 are conducted on CIFAR-FS for 5-way learning using SPAN-ProtoNet.

task interpolation, our framework can achieve a diverse and stable task distribution even when constrained by limited memory budgets. This suggests that the memory buffer’s effectiveness is not solely dependent on its size but also on how the memory is utilized. The ability to maintain performance with limited memory buffers highlights the real-world applicability of our framework.

Table 5. Effect of the budgets of memory buffer.

Memory Buffer Size (task)	5-way 1-shot		5-way 5-shot	
	PEAK	LAST	PEAK	LAST
1	34.06 ± 0.66	26.08 ± 0.72	48.13 ± 0.76	40.12 ± 0.73
10	39.26 ± 0.73	37.65 ± 0.75	53.99 ± 0.76	50.32 ± 0.76
20	40.80 ± 0.78	40.28 ± 0.79	57.11 ± 0.78	55.69 ± 0.76

Effect of the number of pre-trained models. The effect of varying the number of pre-trained models on our method (SPAN), as well as on RANDOM and AVERAGE baselines, is detailed in Tab. 6. We observed that within a certain range, an increase in the number of pre-trained models positively impacts SPAN’s performance. This suggests that SPAN effectively leverages additional models to enhance its learning capability. However, adding more models damages AVERAGE. The reason why AVERAGE even performs worse than RANDOM is that each pre-trained model trains on different tasks, thus lacking precise correspondence in parameter space. The poor performance of AVERAGE also highlights the challenges when utilizing a large volume of models for practical applications.

Table 6. Effect of the number of pre-trained models.

Method	Number	5-way 1-shot		5-way 5-shot	
		PEAK	LAST	PEAK	LAST
RANDOM	0	28.59 ± 0.56	28.59 ± 0.56	34.77 ± 0.62	34.77 ± 0.62
	10	27.99 ± 0.59	27.99 ± 0.59	36.92 ± 0.67	36.92 ± 0.67
	50	24.05 ± 0.51	24.05 ± 0.51	28.16 ± 0.50	28.16 ± 0.50
AVERAGE	100	23.96 ± 0.53	23.96 ± 0.53	27.04 ± 0.51	27.04 ± 0.51
	10	38.32 ± 0.75	37.14 ± 0.76	49.83 ± 0.74	47.22 ± 0.78
	50	39.15 ± 0.75	38.98 ± 0.76	52.41 ± 0.76	51.27 ± 0.76
SPAN	100	40.80 ± 0.78	40.28 ± 0.79	57.11 ± 0.78	55.69 ± 0.76

Time measure. Tab. 7 illustrates the minimal increase in computational time resulting from the integration of AMS. This efficiency is primarily attributable to the rapid computation of rewards and the straightforward policy optimization on reliability scores.

Table 7. Computational efficiency with AMS integration.

Method	Time costs (h) for 10K iterations
SPAN	2.65
SPAN + AMS	2.70

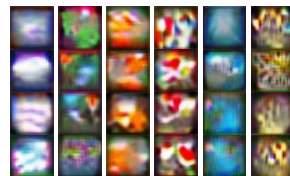


Figure 6. Visualization of data generated from pre-trained Conv4.

Visualization. As depicted in Fig. 6, the pseudo data can effectively recapture the discriminative features learned by pre-trained models, highlighting its suitability for the following meta-learning process.

5. Conclusion

Our work is the first to reveal vulnerabilities of existing inversion-based DFML methods to TDS and TDC, highlighting the urgent necessity to develop robust DFML for real-world applications. In response, we propose a novel DFML framework ensuring task distributional robustness, featuring a pseudo task distribution diversified through task interpolation within a compact memory buffer, and an automated model selection mechanism. Comprehensive experiments verify the effectiveness of our framework in mitigating TDS and TDC, underscoring its potential to deploy DFML for real-world applications.

References

- [1] Luca Bertinetto, Joao F Henriques, Philip HS Torr, and Andrea Vedaldi. Meta-learning with differentiable closed-form solvers. *arXiv preprint arXiv:1805.08136*, 2018. 5, 6, 1
- [2] Kuluhan Binici, Shivam Aggarwal, Nam Trung Pham, Karianto Leman, and Tulika Mitra. Robust and resource-efficient data-free knowledge distillation by generative pseudo replay. In *Proceedings of the AAAI Conference on Artificial Intelligence*, pages 6089–6096, 2022. 3
- [3] Tom Brown, Benjamin Mann, Nick Ryder, Melanie Subbiah, Jared D Kaplan, Prafulla Dhariwal, Arvind Neelakantan, Pranav Shyam, Girish Sastry, Amanda Askell, et al. Language models are few-shot learners. *Advances in neural information processing systems*, 33:1877–1901, 2020. 4
- [4] Hanting Chen, Yunhe Wang, Chang Xu, Zhaohui Yang, Chuanjian Liu, Boxin Shi, Chunjing Xu, Chao Xu, and Qi Tian. Data-free learning of student networks. In *Proceedings of the IEEE/CVF International Conference on Computer Vision*, pages 3514–3522, 2019. 3
- [5] Noel Codella, Veronica Rotemberg, Philipp Tschandl, M Emre Celebi, Stephen Dusza, David Gutman, Brian Helba, Aadi Kallou, Konstantinos Liopyris, Michael Marchetti, et al. Skin lesion analysis toward melanoma detection 2018: A challenge hosted by the international skin imaging collaboration (isic). *arXiv preprint arXiv:1902.03368*, 2019. 7
- [6] Kien Do, Thai Hung Le, Dung Nguyen, Dang Nguyen, Haripriya Harikumar, Truyen Tran, Santu Rana, and Svetha Venkatesh. Momentum adversarial distillation: Handling large distribution shifts in data-free knowledge distillation. *Advances in Neural Information Processing Systems*, 35: 10055–10067, 2022. 3
- [7] Gongfan Fang, Jie Song, Xinchao Wang, Chengchao Shen, Xingen Wang, and Mingli Song. Contrastive model inversion for data-free knowledge distillation. *arXiv preprint arXiv:2105.08584*, 2021.
- [8] Gongfan Fang, Kanya Mo, Xinchao Wang, Jie Song, Shitao Bei, Haofei Zhang, and Mingli Song. Up to 100x faster data-free knowledge distillation. In *Proceedings of the AAAI Conference on Artificial Intelligence*, pages 6597–6604, 2022. 3
- [9] Chelsea Finn, Pieter Abbeel, and Sergey Levine. Model-agnostic meta-learning for fast adaptation of deep networks. In *International conference on machine learning*, pages 1126–1135. PMLR, 2017. 2, 4
- [10] Sebastian Flennerhag, Yannick Schroecker, Tom Zahavy, Hado van Hasselt, David Silver, and Satinder Singh. Bootstrapped meta-learning. In *The Tenth International Conference on Learning Representations*, 2022. 3
- [11] Tim Genewein, Grégoire Delétang, Anian Ruoss, Li Kevin Wenliang, Elliot Catt, Vincent Dutoit, Jordi Grau-Moya, Laurent Orseau, Marcus Hutter, and Joel Veness. Memory-based meta-learning on non-stationary distributions. In *International conference on machine learning*, 2023. 3
- [12] Patrick Helber, Benjamin Bischke, Andreas Dengel, and Damian Borth. Eurosat: A novel dataset and deep learning benchmark for land use and land cover classification. *IEEE Journal of Selected Topics in Applied Earth Observations and Remote Sensing*, 12(7):2217–2226, 2019. 7
- [13] Zixuan Hu, Li Shen, Zhenyi Wang, Tongliang Liu, Chun Yuan, and Dacheng Tao. Architecture, dataset and model-scale agnostic data-free meta-learning. In *Proceedings of the IEEE/CVF Conference on Computer Vision and Pattern Recognition*, 2023. 1, 2, 3, 5, 6
- [14] Huiwon Jang, Hankook Lee, and Jinwoo Shin. Unsupervised meta-learning via few-shot pseudo-supervised contrastive learning. In *The Eleventh International Conference on Learning Representations*, 2023. 3
- [15] Taewon Jeong and Heeyoung Kim. Ood-maml: Meta-learning for few-shot out-of-distribution detection and classification. *Advances in Neural Information Processing Systems*, 33:3907–3916, 2020. 3
- [16] Suhyun Kang, Duhun Hwang, Moonjung Eo, Taesup Kim, and Wonjong Rhee. Meta-learning with a geometry-adaptive preconditioner. In *Proceedings of the IEEE/CVF Conference on Computer Vision and Pattern Recognition*, pages 16080–16090, 2023. 3
- [17] Sanjay Kariyappa, Atul Prakash, and Moinuddin K Qureshi. Maze: Data-free model stealing attack using zeroth-order gradient estimation. In *Proceedings of the IEEE/CVF Conference on Computer Vision and Pattern Recognition*, pages 13814–13823, 2021. 3
- [18] Krishnateja Killamsetty, Changbin Li, Chen Zhao, Rishabh Iyer, and Feng Chen. A reweighted meta learning framework for robust few shot learning. *arXiv preprint arXiv:2011.06782*, 2020. 3
- [19] Brenden M Lake, Ruslan Salakhutdinov, and Joshua B Tenenbaum. Human-level concept learning through probabilistic program induction. *Science*, 350(6266):1332–1338, 2015. 7
- [20] Yann LeCun, Corinna Cortes, and CJ Burges. Mnist handwritten digit database. *ATT Labs [Online]*. Available: <http://yann.lecun.com/exdb/mnist>, 2, 2010. 7
- [21] Hae Beom Lee, Hayeon Lee, Donghyun Na, Saehoon Kim, Minseop Park, Eunho Yang, and Sung Ju Hwang. Learning to balance: Bayesian meta-learning for imbalanced and out-of-distribution tasks. In *ICLR*, 2020. 3

- [22] Aoxue Li, Weiran Huang, Xu Lan, Jiashi Feng, Zhenguo Li, and Liwei Wang. Boosting few-shot learning with adaptive margin loss. In *Proceedings of the IEEE/CVF conference on computer vision and pattern recognition*, pages 12576–12584, 2020. 3
- [23] Bochao Liu, Pengju Wang, Shikun Li, Dan Zeng, and Shiming Ge. Model conversion via differentially private data-free distillation. *arXiv preprint arXiv:2304.12528*, 2023. 3
- [24] Zechun Liu, Zhiqiang Shen, Yun Long, Eric Xing, Kwang-Ting Cheng, and Chas Leichner. Data-free neural architecture search via recursive label calibration. *arXiv preprint arXiv:2112.02086*, 2021.
- [25] Alexander Mordvintsev, Christopher Olah, and Mike Tyka. Inceptionism: Going deeper into neural networks, 2015. 3
- [26] Maria-Elena Nilsback and Andrew Zisserman. Automated flower classification over a large number of classes. In *2008 Sixth Indian conference on computer vision, graphics & image processing*, pages 722–729. IEEE, 2008. 5, 6, 1
- [27] Krunoslav Lehman Pavasovic, Jonas Rothfuss, and Andreas Krause. Mars: Meta-learning as score matching in the function space. In *The Eleventh International Conference on Learning Representations*, 2023. 3
- [28] Matthew Riemer, Ignacio Cases, Robert Ajemian, Miao Liu, Irina Rish, Yuhai Tu, and Gerald Tesauro. Learning to learn without forgetting by maximizing transfer and minimizing interference. *International Conference on Learning Representations*, 2019. 4
- [29] Amrith Setlur, Oscar Li, and Virginia Smith. Two sides of meta-learning evaluation: In vs. out of distribution. *Advances in neural information processing systems*, 34:3770–3783, 2021. 3
- [30] Christian Simon, Piotr Koniusz, and Mehrtash Harandi. Meta-learning for multi-label few-shot classification. In *Proceedings of the IEEE/CVF Winter Conference on Applications of Computer Vision*, pages 3951–3960, 2022. 3
- [31] Jake Snell, Kevin Swersky, and Richard Zemel. Prototypical networks for few-shot learning. *Advances in neural information processing systems*, 30, 2017. 4
- [32] Jihoon Tack, Subin Kim, Sihyun Yu, Jaeho Lee, Jinwoo Shin, and Jonathan Richard Schwarz. Learning large-scale neural fields via context pruned meta-learning. In *Thirty-seventh Conference on Neural Information Processing Systems*, 2023. 3
- [33] Eleni Triantafillou, Tyler Zhu, Vincent Dumoulin, Pascal Lamblin, Utku Evci, Kelvin Xu, Ross Goroshin, Carles Gelada, Kevin Jordan Swersky, Pierre-Antoine Manzagol, and Hugo Larochelle. Meta-dataset: A dataset of datasets for learning to learn from few examples. In *International Conference on Learning Representations*, 2020. 3, 5, 1
- [34] Jean-Baptiste Truong, Pratyush Maini, Robert J Walls, and Nicolas Papernot. Data-free model extraction. In *Proceedings of the IEEE/CVF Conference on Computer Vision and Pattern Recognition*, pages 4771–4780, 2021. 3
- [35] Philipp Tschandl, Cliff Rosendahl, and Harald Kittler. The ham10000 dataset, a large collection of multi-source dermatoscopic images of common pigmented skin lesions. *Scientific data*, 5(1):1–9, 2018. 7
- [36] Oriol Vinyals, Charles Blundell, Timothy Lillicrap, Daan Wierstra, et al. Matching networks for one shot learning. *Advances in neural information processing systems*, 29, 2016. 5, 6, 1
- [37] Risto Vuorio, Shao-Hua Sun, Hexiang Hu, and Joseph J Lim. Multimodal model-agnostic meta-learning via task-aware modulation. *Advances in neural information processing systems*, 32, 2019. 3
- [38] Catherine Wah, Steve Branson, Peter Welinder, Pietro Perona, and Serge Belongie. *The Caltech-UCSD Birds-200-2011 Dataset*. 2011. 5, 6, 1
- [39] Xiaosong Wang, Yifan Peng, Le Lu, Zhiyong Lu, Mohammadhadi Bagheri, and Ronald M Summers. Chestx-ray8: Hospital-scale chest x-ray database and benchmarks on weakly-supervised classification and localization of common thorax diseases. In *Proceedings of the IEEE conference on computer vision and pattern recognition*, pages 2097–2106, 2017. 7
- [40] Zi Wang. Data-free knowledge distillation with soft targeted transfer set synthesis. In *Proceedings of the AAAI Conference on Artificial Intelligence*, pages 10245–10253, 2021. 3
- [41] Zhenyi Wang, Tiehang Duan, Le Fang, Qiuling Suo, and Mingchen Gao. Meta learning on a sequence of imbalanced domains with difficulty awareness. In *Proceedings of the IEEE/CVF International Conference on Computer Vision*, pages 8947–8957, 2021. 3
- [42] Zhenyi Wang, Li Shen, Le Fang, Qiuling Suo, Donglin Zhan, Tiehang Duan, and Mingchen Gao. Meta-learning with less forgetting on large-scale non-stationary task distributions. In *European Conference on Computer Vision*, pages 221–238. Springer, 2022. 3
- [43] Zhenyi Wang, Xiaoyang Wang, Li Shen, Qiuling Suo, Kaiqiang Song, Dong Yu, Yan Shen, and Mingchen Gao. Meta-learning without data via wasserstein distributionally-robust model fusion. In *The 38th Conference on Uncertainty in Artificial Intelligence*, 2022. 1, 3, 5, 6
- [44] Ronald J Williams. Simple statistical gradient-following algorithms for connectionist reinforcement learning. *Reinforcement learning*, pages 5–32, 1992. 5
- [45] Shuo Yang, Lu Liu, and Min Xu. Free lunch for few-shot learning: Distribution calibration. *arXiv preprint arXiv:2101.06395*, 2021. 3
- [46] Huaxiu Yao, Xian Wu, Zhiqiang Tao, Yaliang Li, Bolin Ding, Ruirui Li, and Zhenhui Li. Automated relational meta-learning. In *International Conference on Learning Representations*, 2020. 3
- [47] Huaxiu Yao, Yu Wang, Ying Wei, Peilin Zhao, Mehrdad Mahdavi, Defu Lian, and Chelsea Finn. Meta-learning with an adaptive task scheduler. *Advances in Neural Information Processing Systems*, 34:7497–7509, 2021. 3
- [48] Huaxiu Yao, Linjun Zhang, and Chelsea Finn. Meta-learning with fewer tasks through task interpolation. In *Proceeding of the 10th International Conference on Learning Representations*, 2022. 4
- [49] Han-Jia Ye, Lu Ming, De-Chuan Zhan, and Wei-Lun Chao. Few-shot learning with a strong teacher. *IEEE Transactions on Pattern Analysis and Machine Intelligence*, 2022. 3

- [50] Hongxu Yin, Pavlo Molchanov, Jose M Alvarez, Zhizhong Li, Arun Mallya, Derek Hoiem, Niraj K Jha, and Jan Kautz. Dreaming to distill: Data-free knowledge transfer via deep-inversion. In *Proceedings of the IEEE/CVF Conference on Computer Vision and Pattern Recognition*, pages 8715–8724, 2020. 4
- [51] Runsheng Yu, Weiyu Chen, Xinrun Wang, and James Kwok. Enhancing meta learning via multi-objective soft improvement functions. In *The Eleventh International Conference on Learning Representations*, 2023. 3
- [52] Shikang Yu, Jiachen Chen, Hu Han, and Shuqiang Jiang. Data-free knowledge distillation via feature exchange and activation region constraint. In *Proceedings of the IEEE/CVF Conference on Computer Vision and Pattern Recognition*, pages 24266–24275, 2023. 3
- [53] Jie Zhang, Chen Chen, Bo Li, Lingjuan Lyu, Shuang Wu, Shouhong Ding, Chunhua Shen, and Chao Wu. Dense: Data-free one-shot federated learning. *Advances in Neural Information Processing Systems*, 35:21414–21428, 2022. 3
- [54] Lin Zhang, Li Shen, Liang Ding, Dacheng Tao, and Ling-Yu Duan. Fine-tuning global model via data-free knowledge distillation for non-iid federated learning. In *Proceedings of the IEEE/CVF Conference on Computer Vision and Pattern Recognition*, pages 10174–10183, 2022. 3
- [55] Yiman Zhang, Hanting Chen, Xinghao Chen, Yiping Deng, Chunjing Xu, and Yunhe Wang. Data-free knowledge distillation for image super-resolution. In *Proceedings of the IEEE/CVF Conference on Computer Vision and Pattern Recognition*, pages 7852–7861, 2021. 3
- [56] Zhuangdi Zhu, Junyuan Hong, and Jiayu Zhou. Data-free knowledge distillation for heterogeneous federated learning. In *International Conference on Machine Learning*, pages 12878–12889. PMLR, 2021. 3

Task-Distributionally Robust Data-Free Meta-Learning

Supplementary Material

A. Additional Experimental Setup

Our experiments utilized four datasets: CIFAR-FS [1], MiniImageNet [36], VGG-Flower [26], and CUB-200-2011 (CUB) [38], ranging from general natural images to specific categories like birds (CUB) and flowers (VGG-Flower). Following standard splits [33], we split each dataset into meta-training, meta-validating and meta-testing subsets with disjoint label spaces. Following Wang et al. [43] and Hu et al. [13], we collect 100 models pre-trained on 100 N -way tasks sampled from the meta-training subset, while the meta-learner is finally evaluated on 600 tasks sampled from the meta-testing subset. Those pre-trained models are trained using an Adam optimizer with a learning rate of 0.01 for 60 epochs. The meta-learner and pre-trained models employ a Conv4 architecture for consistency with existing works. Conv4 consists of four convolutional blocks. Each block consists of 32 3×3 filters, a BatchNorm, a ReLU and a 2×2 max-pooling. Hyperparameters included an inner learning rate of 0.01 and an outer learning rate of 0.001 for SPAN-ANIL, and a learning rate of 0.001 for SPAN-ProtoNet. The threshold p_s is empirically set as 0.4. α and β of the Beta distribution are set as 0.5. The memory bank was limited to 20 tasks. For generator training, we adopt Adam optimizer with a learning rate of 0.001 for 200 epochs with its structure detailed in Tab. 8. If not otherwise specified, we use *combination* for task interpolation. All experiments are conducted on one NVIDIA GeForce RTX 3090 GPU.

B. Additional Algorithm

Alg. 2 outlines the task-generation algorithm described in Eq. (4). To construct the pseudo task $\hat{\mathcal{T}}$, we select $\hat{\mathbf{X}}$ that yields the minimum \mathcal{L}_G during the optimization of θ_G , and then randomly split $(\hat{\mathbf{X}}, \hat{\mathbf{Y}})$ into a support set $\hat{\mathbf{D}}^s = (\hat{\mathbf{X}}^s, \hat{\mathbf{Y}}^s)$ and a query set $\hat{\mathbf{D}}^q = (\hat{\mathbf{X}}^q, \hat{\mathbf{Y}}^q)$.

Algorithm 2: Subroutine of task generation

```
1 Input: Max iterations  $N_G$  for task generation; the pre-trained model  $M$  and the corresponding generator  $G(\cdot; \theta_G)$ .
2 Function TaskGeneration( $M, G$ ):
3   Initialize  $minLoss \leftarrow +\infty$ ,  $bestTask \leftarrow None$ 
4   Randomly initialize  $\theta_G$ 
5   Set the target labels  $\mathbf{Y}$ 
6   for each iteration  $n_g \leftarrow 1$  to  $N_G$  do
7     Randomly sample a batch of noise  $\mathbf{Z}$  from the standard Gaussian distribution
8      $\mathbf{X}^{(n_g)} \leftarrow G(\mathbf{Z}, \mathbf{Y}; \theta_G^{(n_g)})$ 
9     Calculate the loss value  $\mathcal{L}_G^{(n_g)} \leftarrow \mathcal{L}_G(\mathbf{Z}, \mathbf{Y}; \theta_G^{(n_g)})$ 
10     $\theta_G^{(n_g+1)} \leftarrow \theta_G^{(n_g)} - \nabla_{\theta_G} \mathcal{L}_G^{(n_g)}$  (Eq. (4))
11    if  $\mathcal{L}_G^{(n_g)} < minLoss$  then
12       $minLoss \leftarrow \mathcal{L}_G^{(n_g)}$ 
13       $bestTask \leftarrow \mathbf{X}^{(n_g)}$ 
14  Randomly split  $bestTask$  into the support set  $\hat{\mathbf{D}}^s$  and the query set  $\hat{\mathbf{D}}^q$ 
15  return  $bestTask$  with  $\hat{\mathbf{D}}^s$  and  $\hat{\mathbf{D}}^q$ 
```

C. Architecture of Conditional Generator

Tab. 8 lists the structure of the conditional generator in our proposed SPAN. The generator takes the standard Gaussian noise and the one-hot label embedding as inputs and outputs the generated data. Here, d_z is the dimension of Gaussian noise data \mathbf{z} , which is set as 256 in practice. We set *img_size* as 32. We set the number of channels *nc* as 3 for color image recovery and the number of convolutional filters *nf* as 64.

Table 8. Detailed structure of conditional generator. We highlight the dimension change in blue.

Notion	Description	
$img_size \times img_size$	resolution of generated image	
bs	batch size	
nc	number of channels of generated image	
nf	number of convolutional filters	
FC(-)	fully connected layer;	
BN(-)	batch normalization layer	
Conv2D(input, output, filter_size, stride, padding)	convolutional layer	

Structure	Dimension	
	Before	After
$z \in \mathbb{R}_{d_z} \sim \mathcal{N}(0, 1)$	—	$[bs, d_z]$
$y \in \mathbb{R}_{d_y}$	—	$[bs, d_y]$
FC ₁ (z)	$[bs, d_z]$	$[bs, nf \times (img_size//4) \times (img_size//4)]$
FC ₂ (y)	$[bs, d_y]$	$[bs, nf \times (img_size//4) \times (img_size//4)]$
Concatenate(FC ₁ (z), FC ₂ (y))	—	$[bs, 2 \times nf \times (img_size//4) \times (img_size//4)]$
Reshape	$[bs, 2 \times nf \times (img_size//4) \times (img_size//4)]$	$[bs, 2 \times nf, (img_size//4), (img_size//4)]$
BN	$[bs, 2 \times nf, (img_size//4), (img_size//4)]$	$[bs, 2 \times nf, (img_size//4), (img_size//4)]$
Upsampling	$[bs, 2 \times nf, (img_size//4), (img_size//4)]$	$[bs, 2 \times nf, (img_size//2), (img_size//2)]$
Conv2D($2 \times nf, 2 \times nf, 3, 1, 1$)	$[bs, 2 \times nf, (img_size//2), (img_size//2)]$	$[bs, 2 \times nf, (img_size//2), (img_size//2)]$
BN, LeakyReLU	$[bs, 2 \times nf, (img_size//2), (img_size//2)]$	$[bs, 2 \times nf, (img_size//2), (img_size//2)]$
Upsampling	$[bs, 2 \times nf, (img_size//2), (img_size//2)]$	$[bs, 2 \times nf, img_size, img_size]$
Conv2D($2 \times nf, nf, 3, 1, 1$)	$[bs, 2 \times nf, img_size, img_size]$	$[bs, nf, img_size, img_size]$
BN, LeakyReLU	$[bs, nf, img_size, img_size]$	$[bs, nf, img_size, img_size]$
Conv2D($nf, nc, 3, 1, 1$)	$[bs, nf, img_size, img_size]$	$[bs, nc, img_size, img_size]$
Sigmoid	$[bs, nc, img_size, img_size]$	$[bs, nc, img_size, img_size]$

D. Additional Discussions

Take a closer look at PURER. The state-of-the-art method, PURER [13], trains a meta-learner on pseudo tasks constructed from a learnable dataset. This learnable dataset is inversely generated from the pre-trained model pool and also adversarially evolves alongside the meta-learner. The overall objective of PURER is shown in the equation below:

$$\min_{\theta} \max_{\mathcal{D}} \mathbb{E}_{\mathcal{T} \in \mathcal{D}} [-\mathcal{L}_{\text{data}}(\mathcal{D}) + \mathcal{L}_{\text{meta}}(\mathcal{T}; \theta)]$$

Vulnerability to TDS. The learnable dataset \mathcal{D} is optimized simultaneously with two terms: (i) minimizing the data-generation loss $\mathcal{L}_{\text{data}}$ and (ii) maximizing the meta-learning loss $\mathcal{L}_{\text{meta}}$. $\mathcal{L}_{\text{data}}$ is implemented via the cross-entropy loss, which is minimized to ensure the generated data can be correctly classified as the pre-defined labels. To further generate increasingly challenging tasks for the meta-learner, PURER optimizes \mathcal{D} by maximizing $\mathcal{L}_{\text{meta}}$. This makes the generated tasks with higher meta-learning loss, *i.e.* they can not be well solved by the current meta-learner. The evolving nature of the learnable dataset \mathcal{D} leads to shifts in the distribution of pseudo tasks. As PURER trains the learnable dataset and meta-learner adversarially, these shifts can be substantial, potentially biasing the meta-learner towards newly generated tasks and away from an ideal task distribution.

Vulnerability to TDC. PURER assumes the trustworthiness of all pre-trained models, generating pseudo data from the entire model pool without discrimination. In real-world scenarios, models from public repositories are not always trusted. Untrusted or poisoned models can be uploaded by users or even attackers without restrictions. Here, we identify two primary risks with untrusted models: those with misleading labels, either due to inaccurate data labeling or deliberate model disguising, and those of low quality, stemming from poor training configurations or inferior training data. Specifically, (i) pseudo data generated from models with misleading labels will be inaccurately labeled, causing contradictions with correctly labeled data and thus confusing the meta-learner. We use an example of model disguise: given Mars-Jupiter classifier deceptively claimed as a dog-cat classifier, the true “Mars” images generated from it will be falsely labeled as “dog”, contradicting with the true “dog” and other false “dog” images, which thus confuses the meta-learner; even there is no contradiction, the false “dog” images still cause a huge distribution gap (*i.e.*, the original distribution gap between “Mars” and animal images). (ii) Likewise, data generated from low-quality models are often noisy and lacking in discriminative features, thereby hindering the meta-learning process. The main objective of data generation is to “invert” data with low classification loss. Therefore, if the model can not recognize the “dog”, we can not generate the discriminative features from it.

Addressing this issue by individually assessing each model’s reliability through gathering specific testing data, though straightforward, is impractical in DFML scenarios, given the vast number of pre-trained models and associated constraints like time, resources, and privacy. Therefore, we advocate for the development of an efficient, automated method to identify and utilize reliable models from a large pool without necessitating extensive individual model testing.

E. Additional Experiments

General versatility of AMS. To further demonstrate the versatility of our proposed AMS, we integrate it to PURER [13] on CIFAR-FS for 5-way 1-shot and 5-shot learning. AMS consistently improves PURER’s performance under varying degrees of model pollution (20% and 40%). Specifically: For a pollution rate of 20%, AMS enhancement results in an increase of 1.48% in 5-way 1-shot learning (from 35.52% to 37.00%) and 2.02% in 5-way 5-shot learning (from 50.16% to 52.18%). With a 40% pollution rate, the performance gains are 1.55% in 5-way 1-shot learning (from 35.37% to 36.92%) and 1.86% in 5-way 5-shot learning (from 48.3% to 50.25%). These results indicate its general versatility for improving the robustness of existing DFML methods in real-world scenarios with untrusted models.

Table 9. General versatility of AMS.

Pollution Rate	Method	5-way 1-shot	5-way 5-shot
20%	PURER	35.52 ± 0.55	50.16 ± 0.64
	PURER + AMS	37.00 ± 0.62 _{+1.48%}	52.18 ± 0.65 _{+2.02%}
40%	PURER	35.37 ± 0.64	48.39 ± 0.63
	PURER + AMS	36.92 ± 0.55 _{+1.55%}	50.25 ± 0.66 _{+1.86%}

Model-agnostic nature of our framework. In order to illustrate the model-agnostic nature of our proposed framework, we conduct experiments using different neural network architectures on CIFAR-FS. The results, as shown in Tab. 10, indicate how our framework performs across varied architectures in both 5-way 1-shot and 5-way 5-shot learning scenarios. With a homogeneous architecture (100% Conv4), the framework achieves 40.80% in 5-way 1-shot learning and 57.11% in 5-way 5-shot learning. In a heterogeneous setting, comprising 33% Conv4, 33% ResNet10, and 33% ResNet18, the framework attains 41.94% in 5-way 1-shot learning and 57.02% in 5-way 5-shot learning. These findings demonstrate that our framework maintains consistent performance regardless of the underlying neural network architectures, indicating its effective model-agnostic properties.

Table 10. Model-agnostic nature of our framework.

Architecture	5-way 1-shot		5-way 5-shot	
	PEAK	LAST	PEAK	LAST
100% Conv4	40.80 ± 0.78	40.28 ± 0.79	57.11 ± 0.78	55.69 ± 0.76
33% Conv4 + 33% ResNet10 + 33% ResNet18	41.94 ± 0.73	41.56 ± 0.74	57.02 ± 0.76	56.04 ± 0.75

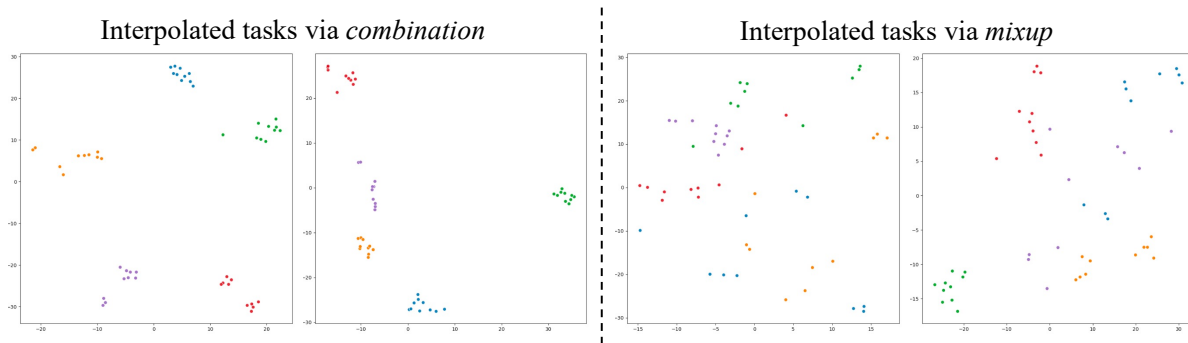


Figure 7. T-SNE visualization of interpolated tasks.

T-SNE visualization of interpolated tasks. The t-SNE visualization in Fig. 7 provides insights into the effectiveness of task interpolation methods used in our experiments. The left panel displays interpolated tasks via combination, where each color represents a different task, and points represent individual examples within those tasks. The combination method shows distinct clusters, indicating that tasks are well-separated in the feature space, which could be beneficial for the meta-learner to distinguish between tasks.

The right panel shows interpolated tasks via mixup. Here, we observe a more blended distribution of points, suggesting that mixup creates tasks with overlapping features. This overlap can be advantageous for the meta-learner by introducing a gradient of difficulty levels and promoting better generalization.

A hybrid approach, utilizing both combination and mixup, yields superior performance as it benefits from the diversity of the more distinctly separated tasks (from combination) and the nuanced, complex tasks that challenge the meta-learner’s generalization capabilities (from mixup). This is supported by empirical results detailed in Tab. 4, where the hybrid approach demonstrates enhanced performance due to a richer variety of tasks with varying difficulty levels, a desirable property for robust meta-learning.

AMS against low-quality models. Additional experiments are conducted on CIFAR-FS to assess the effectiveness of AMS against low-quality models—specifically, those with testing accuracies below 25%. These experiments, to be elaborated in Tab. 11, show the application of AMS to the SPAN method under varying rates of model pollution. For 5-way 1-shot learning, AMS increases SPAN’s performance by 1.03% at a 20% pollution rate and by 1.55% at a 40% pollution rate. For 5-way 5-shot learning, the performance gains are 1.87% and 2.06% at pollution rates of 20% and 40%, respectively. These results confirm that AMS consistently enhances the robustness of DFML methods, such as SPAN, by effectively mitigating the impact of low-quality models within the training pool.

Table 11. AMS against low-quality models.

Pollution Rate	Method	5-way 1-shot	5-way 5-shot
20%	SPAN	34.54 ± 0.72	48.72 ± 0.78
	SPAN + AMS	35.57 ± 0.71 +1.03%	50.59 ± 0.76 +1.87%
40%	SPAN	34.02 ± 0.72	45.68 ± 0.73
	SPAN + AMS	35.37 ± 0.73 +1.55%	47.74 ± 0.74 +2.06%